B.Tech Project Presentation

Pulse Electrodeposition of CuO/Cu_2O on 3D-Printed Nickel-Containing Carbon Structures for Visible-Light-Driven Photocatalytic Degradation of Methylene Blue

Presented by:
Ojasvi Pandey(B22ME043)
Nikita Sewda(B22ME042)

Department of Mechanical Engineering
Indian Institute of Technology,Jodhpur

Motivation

In India , 820 million people face high to extreme water stress

200,000 Indians die annually due to inadequate water quality

By 2030, 700 million people could be displaced due to water scarcity

The Hidden Poison: Methylene Blue Contamination

- Tissue necrosis (the death of body tissue)
- Cyanosis (oxygen deprivation causing Blue skin discoloration)
- Respiratory distress
- Cardiovascular complications
- Vomiting
- Jaundice
- Neurological damage
- Carcinogenic
- Mutagenic
- Highly toxic

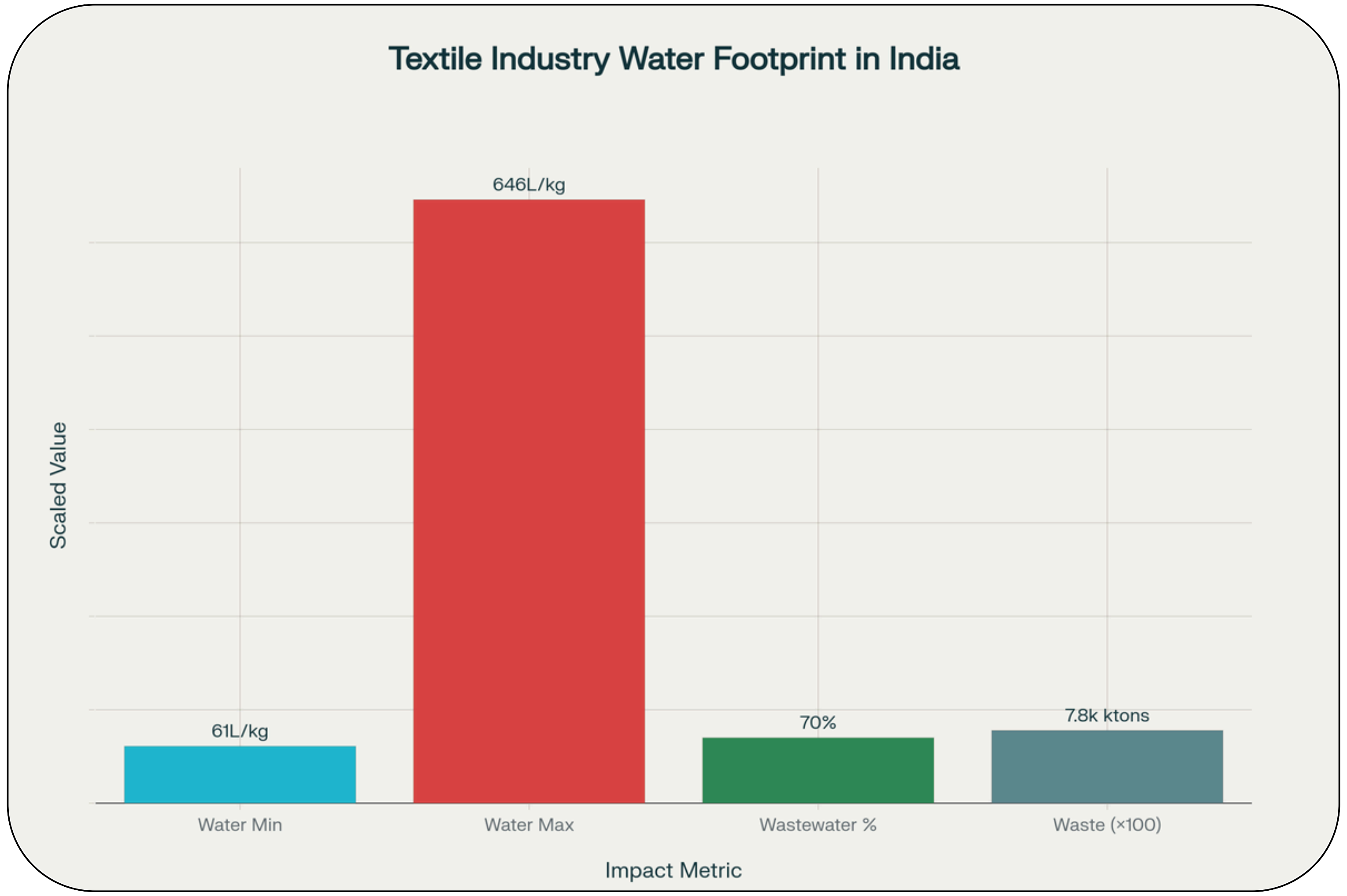

Visual representation of the textile industry's massive water consumption and pollution footprint in India

Objective

To compare the photocatalytic performance of 3D-PEGDA/x%Ni_Cu_2O and 3D-PEGDA/x%Ni_Cu_2O_Ag microlattice structures for efficient degradation of methylene blue in water.

Advantages pyrolytic carbon structure designed as a microlattice

- The microlattice design allows UV light to penetrate deep into the 3D-PEGDA/x%Ni_Cu_2O_Ag structure, maximizing photon absorption and uniform ROS generation.
- Its 3D porous geometry offers a high surface area for greater catalyst loading and more active sites, enhancing pollutant degradation efficiency.

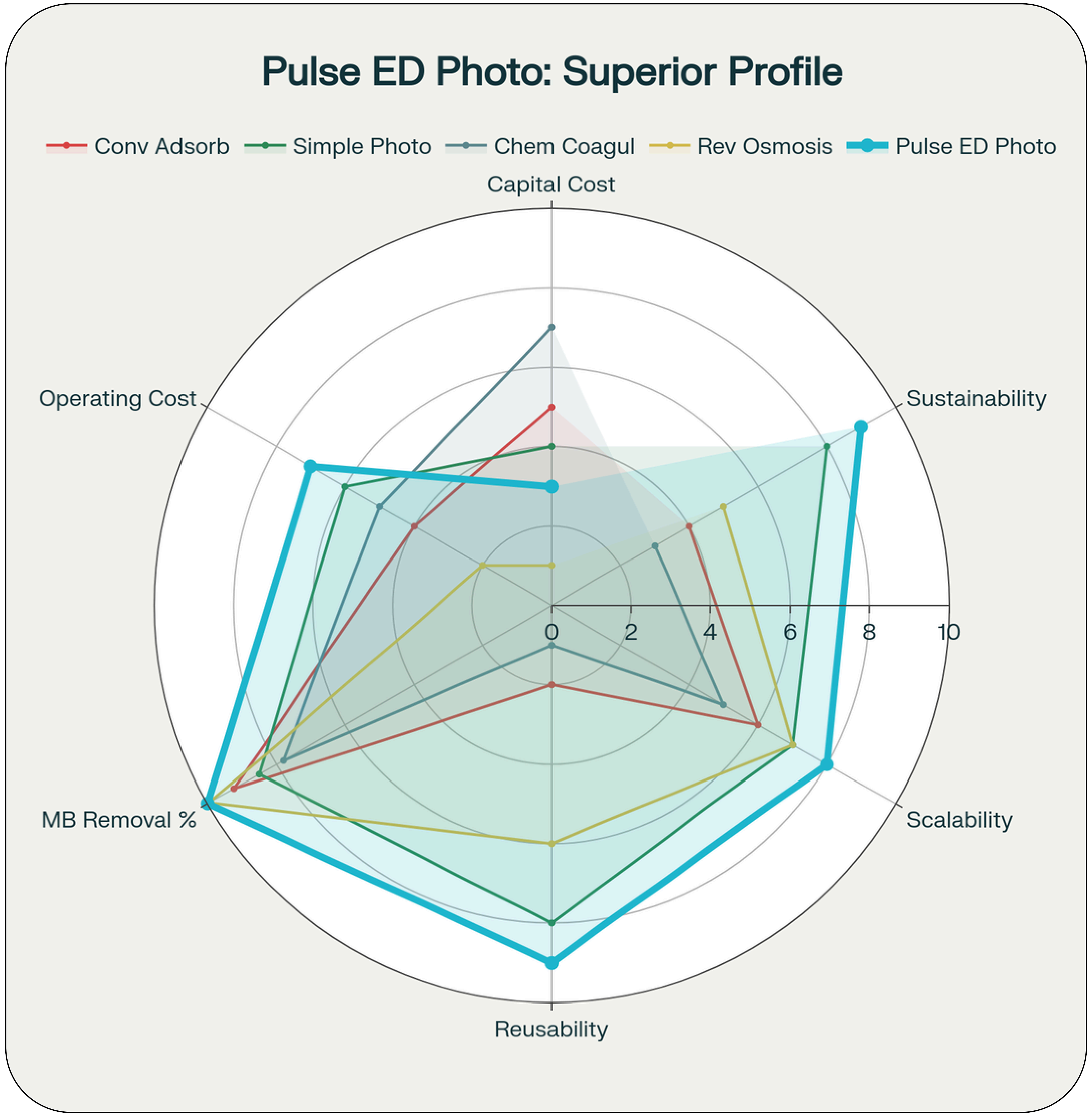

Sources :

Source 1 Source 2 Source 3

Source 4 Source 5 Source 6

Photocatalytic Breakdown Process

1) Photon absorption — generating charge carriers:

$Cu_2O + h\nu \rightarrow e^-$ (CB) + h^+ (VB)

2) Charge separation & transfer (role of Ag NW and PyC):

e^- (CB, Cu_2O) → e^- (Ag or PyC) (electron transfer to Ag or PyC)

Ag + $h\nu$ → Ag*(hot electron) → inject e^- (plasmonic hot-electron injection; optional extra path)

3) Oxygen reduction → superoxide radical

$O_2 + e^- \rightarrow \bullet O_2^-$ (superoxide radical anion)

4) Protonation / disproportionation → hydroperoxyl ($HO_2\bullet$) and hydrogen peroxide (H_2O_2)

$\bullet O_2^- + H^+ \rightarrow HO_2\bullet$ (protonation to hydroperoxyl radical)

$2\ \bullet O_2^- + 2\ H^+ \rightarrow H_2O_2 + O_2$ (disproportionation / dismutation)

$HO_2\bullet + e^- + H^+ \rightarrow H_2O_2$ (reduction of $HO_2\bullet$ to hydrogen peroxide)

5) Hydrogen peroxide → hydroxyl radical

Two main routes:

Reduction by electron:

$H_2O_2 + e^- \rightarrow \bullet OH + OH^-$

Photolysis (light-induced):

$H_2O_2 + h\nu \rightarrow 2\ \bullet OH$

6) Catalyzed decomposition on metal surfaces:

$H_2O_2 \rightarrow 2\ \bullet OH$ (Ag surface may catalyze decomposition under certain conditions)

Direct hole oxidation (alternate path):

$h^+ + OH^- \rightarrow \bullet OH$

$h^+ + H_2O \rightarrow \bullet OH + H^+$

7) Overall pollutant oxidation / mineralization

Representative overall step:

R (organic) + $\bullet OH$ / h^+ / $\bullet O_2^-$ → oxidized intermediates → $CO_2 + H_2O$

Preparation of samples

Design and Fabrication

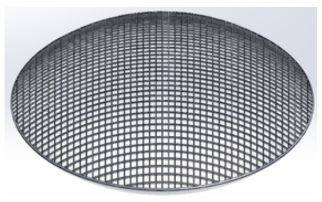

CAD Model

.STL File

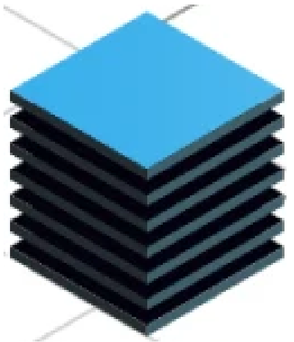

Slicing

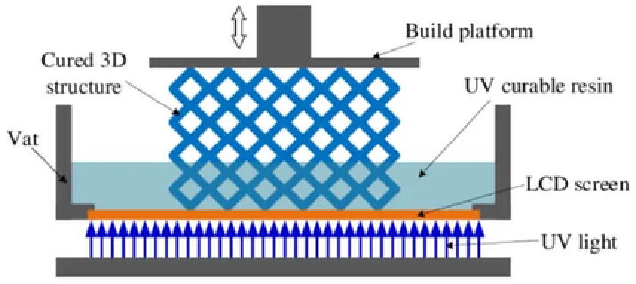

DLP 3D Printing

Pyrolysis@900 °C

3D Pyrolytic Carbon Substrate

Electrochemical Deposition

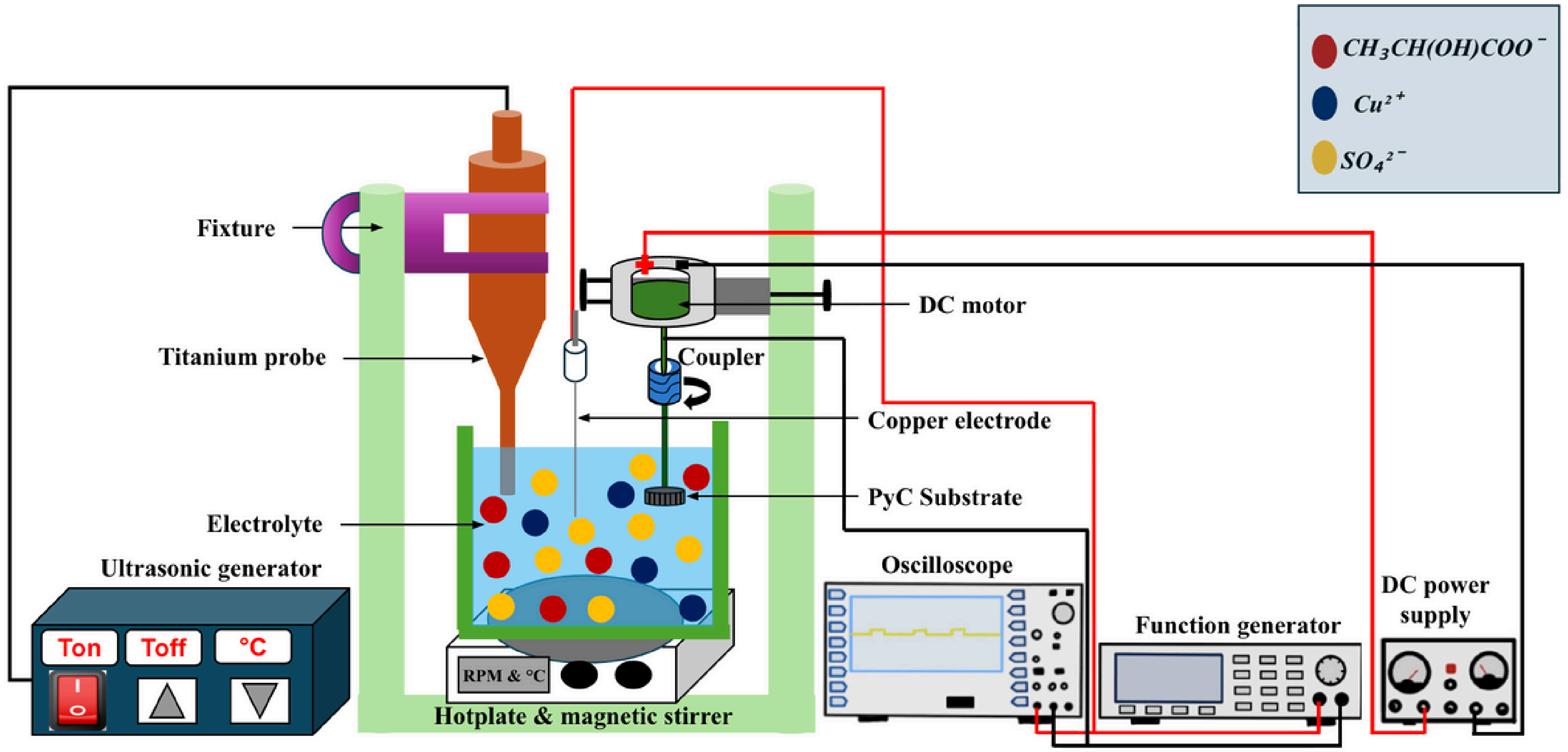

Parameters-

Frequency- 50Hz

Volatge- 5V

Duty Cycle- 40%

Electrolyte Composition-

NaOH - 1.6%

$CuSO_4{\cdot}5H_2O$ - 0.75%

Lactic acid - 3.9%

Drop Casting

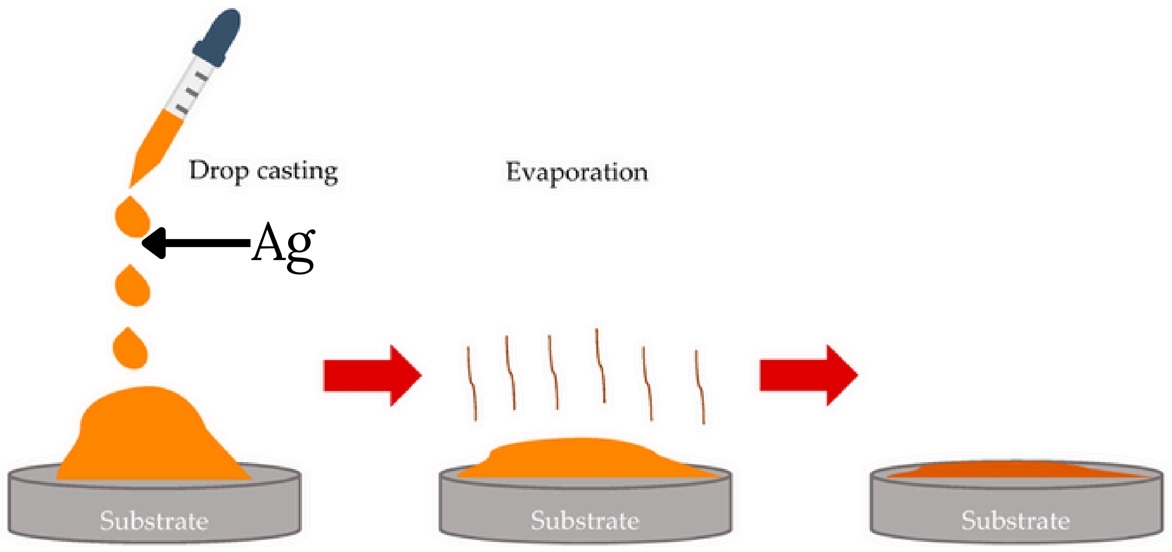

Characterization

SEM

SEM is used to study the surface morphology and microstructural features of the microlattice. It provides general insights into the overall structure, including the deposition and distribution of Cu_2O and Ag on the pyrolytic carbon surface.

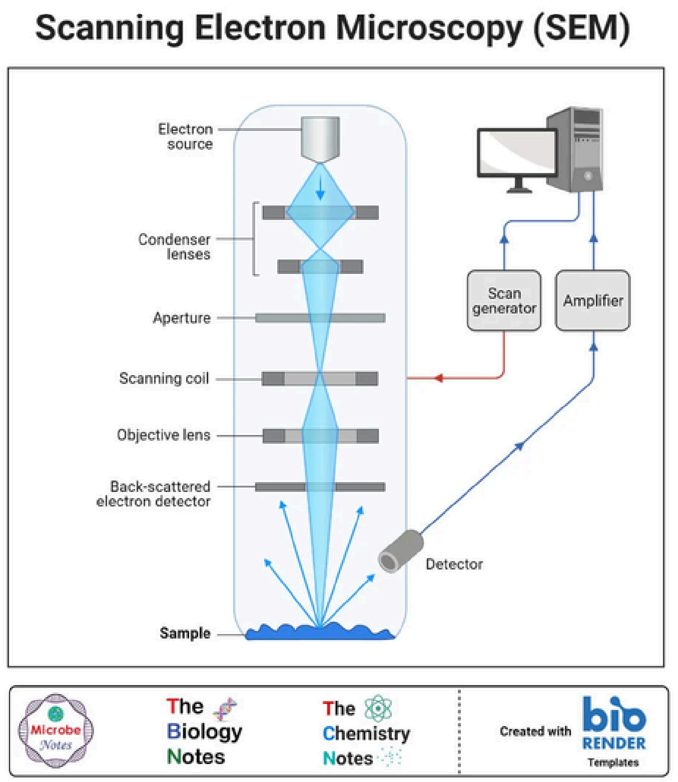

FESEM

FESEM is also used to study the surface morphology and microstructural features, offering higher resolution and clearer surface details compared to conventional SEM. This allows for a more precise analysis of the deposition and distribution of Cu_2O and Ag on the pyrolytic carbon surface.

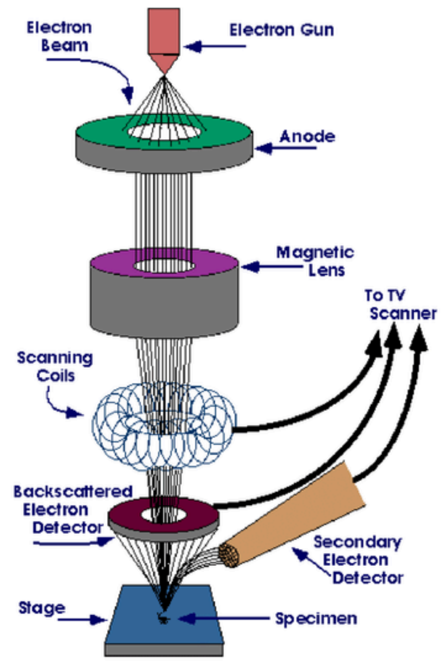

EDS

EDS (Energy Dispersive X-ray Spectroscopy) is used to determine the elemental composition of a material and to confirm the presence and distribution of elements like Cu, O, Ag, Ni, and C in the synthesized photocatalyst.

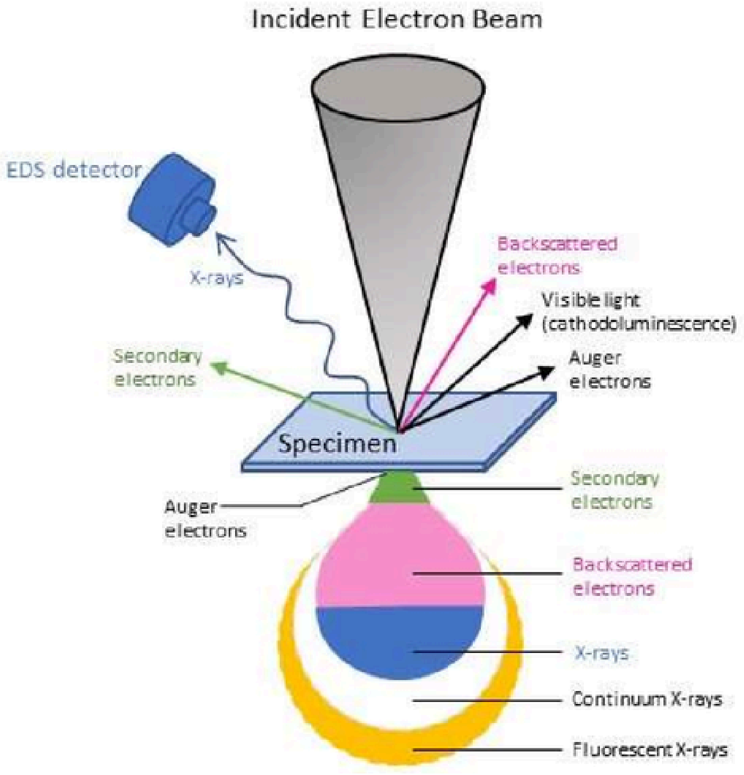

XRD

XRD (X-ray Diffraction) is used to identify the crystalline phases present in a material and to determine its crystal structure, purity, and average crystallite size, confirming the formation of compounds like Cu_2O and Ag on the pyrolytic carbon framework.

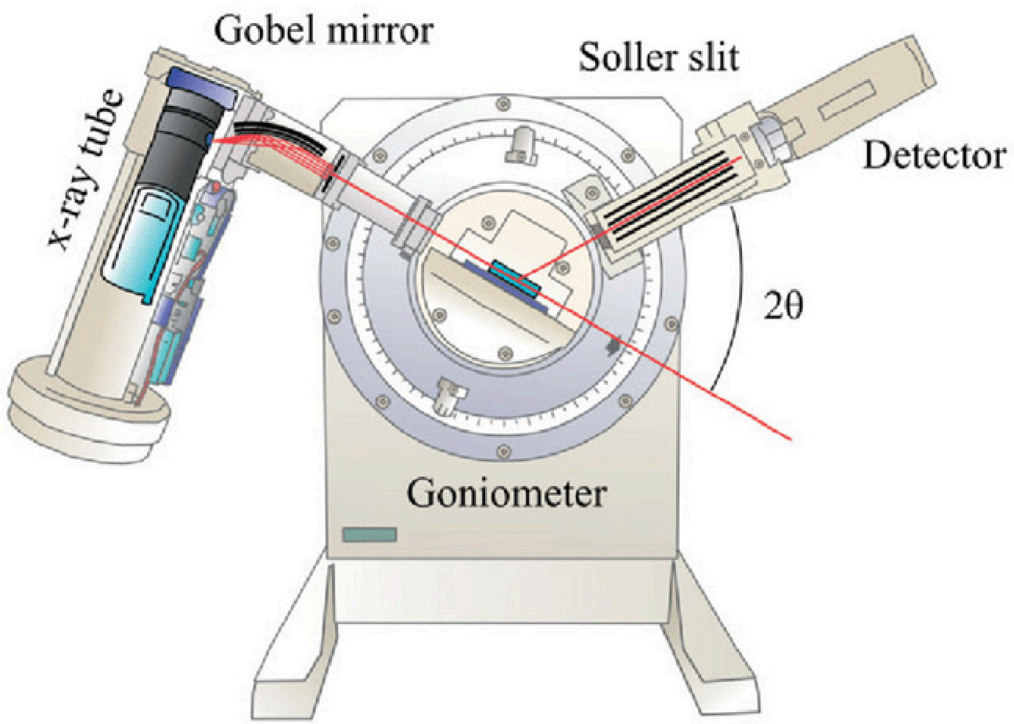

Characterization

Raman Spectroscopy

Raman Spectroscopy is a non-destructive technique used to characterize the chemical structure and molecular vibrations of the material. For the Cu_2O and Ag deposited on the pyrolytic carbon microlattice, it specifically helps to identify the different phases present (e.g., confirming Cu_2O and Ag particles) and provides crucial structural insights.

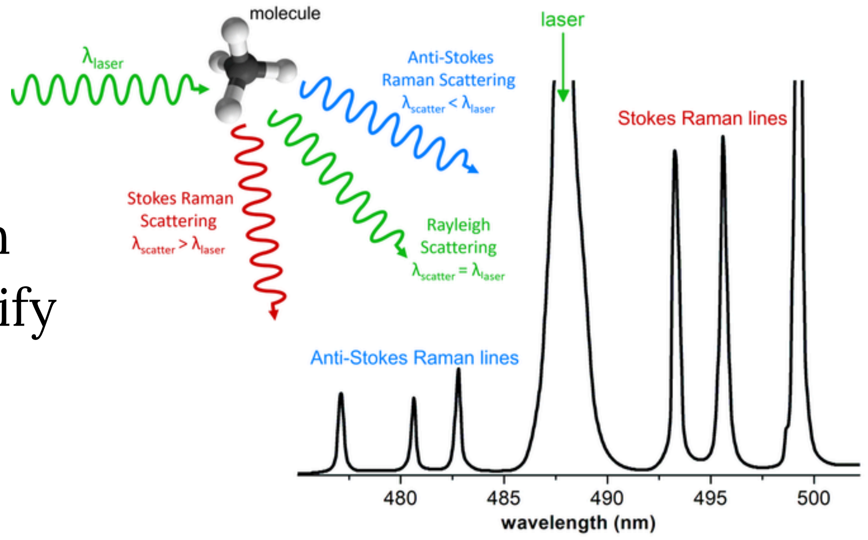

UV-Vis Spectroscopy

UV-Vis Spectroscopy is used to study the optical properties of the photocatalyst, such as light absorption and band gap energy, helping to evaluate its photocatalytic efficiency and ability to absorb UV or visible light for dye degradation.

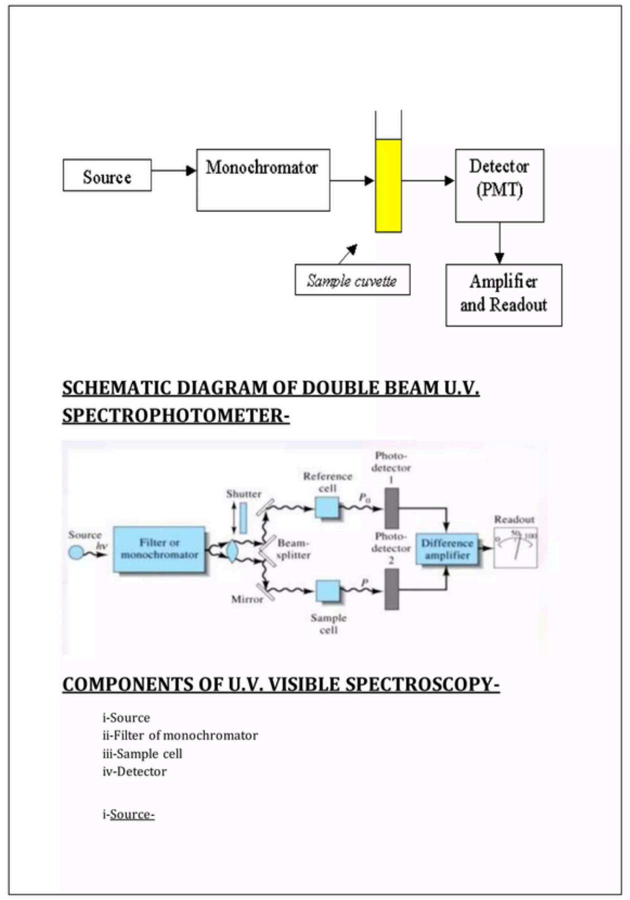

Source → Monochromator → Detector (PMT)

Sample cuvette

Amplifier and Readout

SCHEMATIC DIAGRAM OF DOUBLE BEAM U.V. SPECTROPHOTOMETER-

COMPONENTS OF U.V. VISIBLE SPECTROSCOPY-

i-Source
ii-Filter of monochromator
iii-Sample cell
iv-Detector

i-Source-

Sample

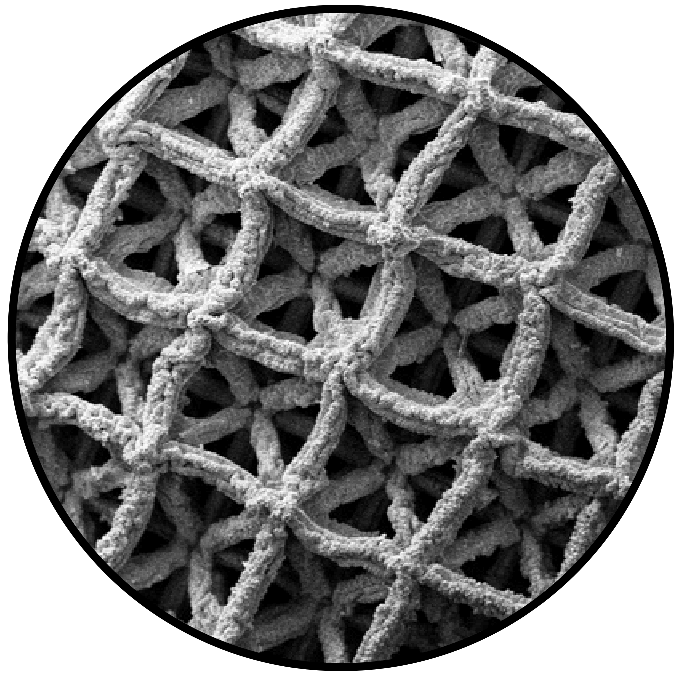

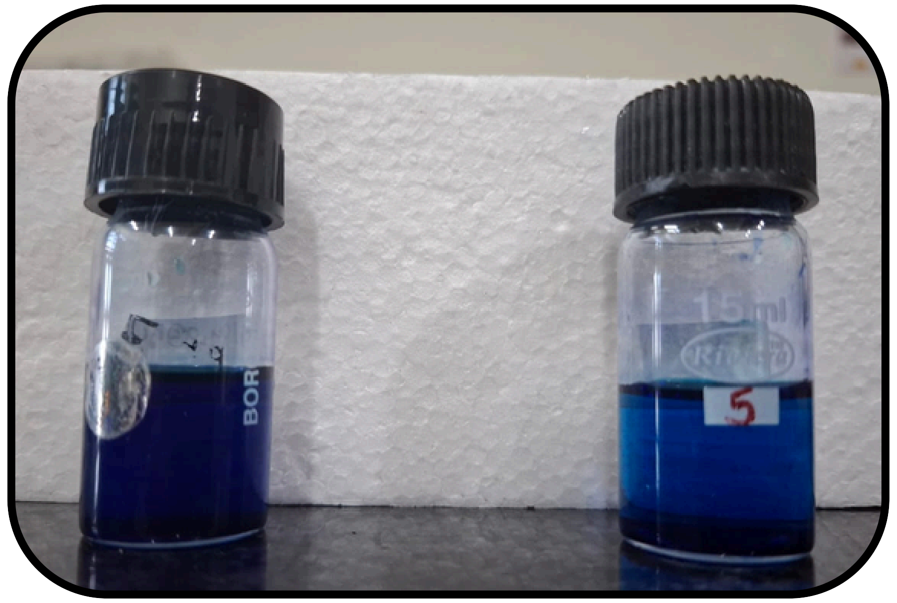

SEM

3D-PEGDA/0.5Ni_Cu_2O

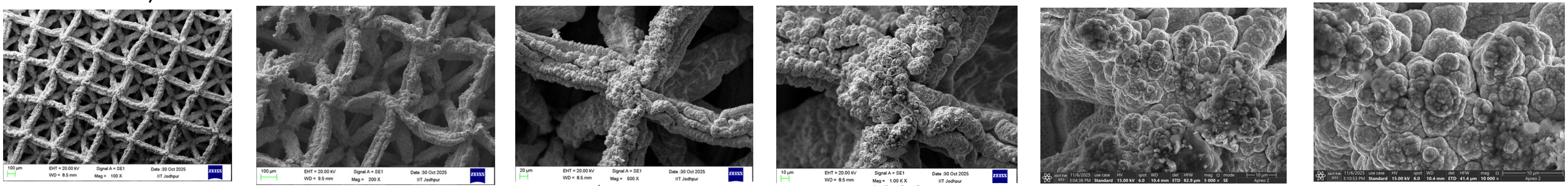

100x 200x 500x 1000x 5000x 10000x

3D-PEGDA/1Ni_Cu_2O

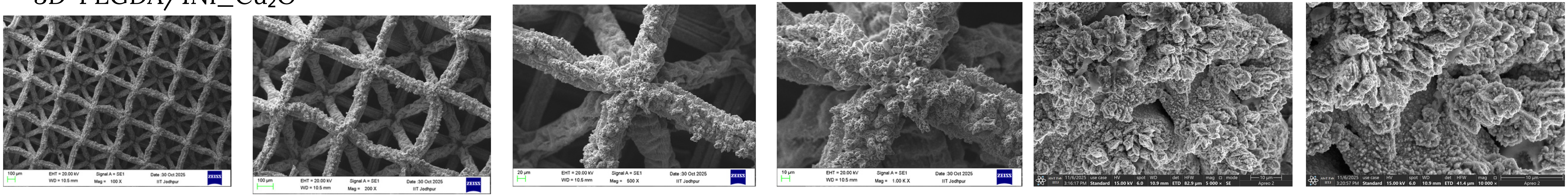

3D-PEGDA/5Ni_Cu_2O

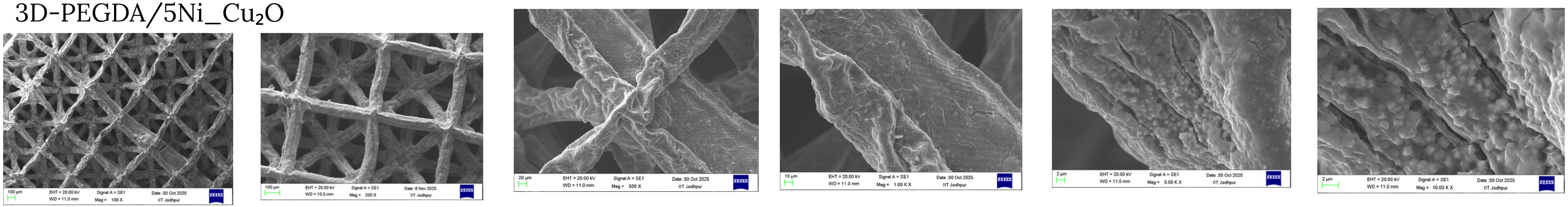

3D-PEGDA/10Ni_Cu_2O

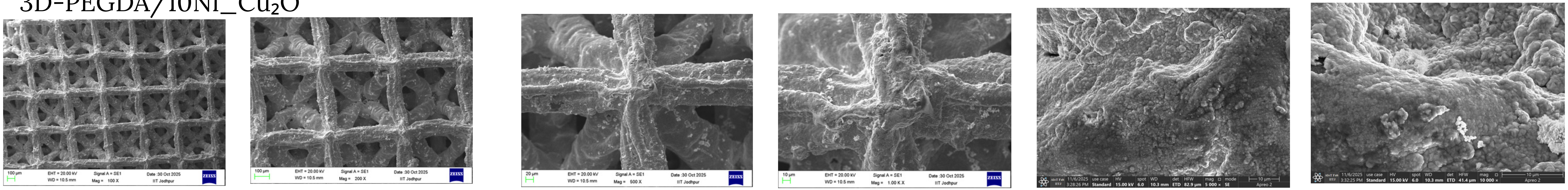

3D-PEGDA/0.5Ni_Cu_2O_Ag

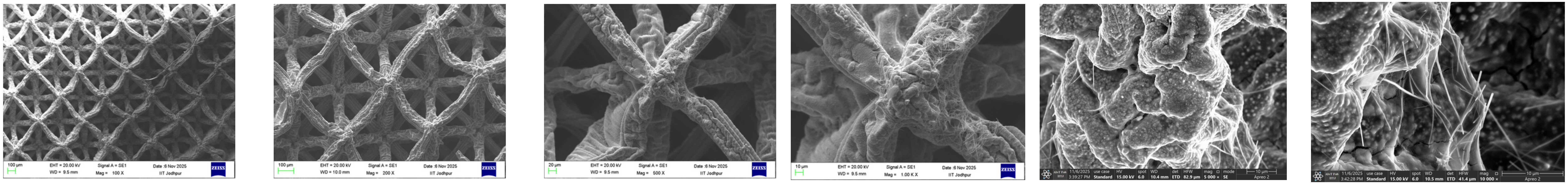

3D-PEGDA/1Ni_Cu_2O_Ag

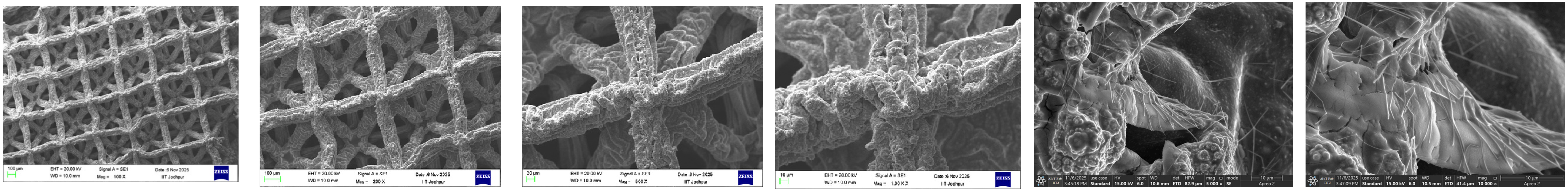

3D-PEGDA/5Ni_Cu_2O_Ag

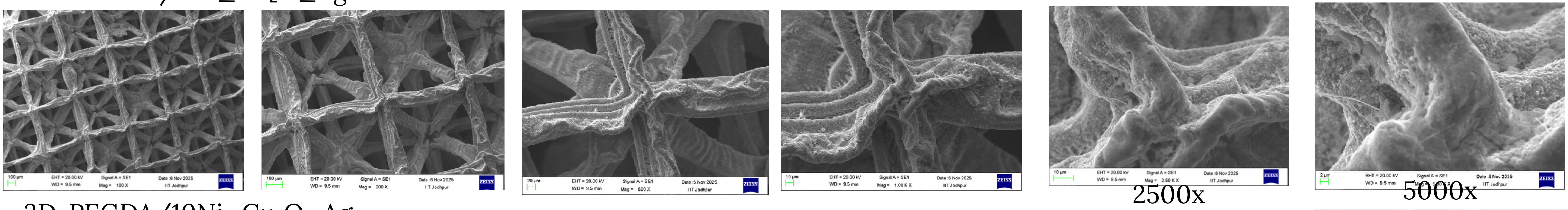

3D-PEGDA/10Ni_Cu_2O_Ag

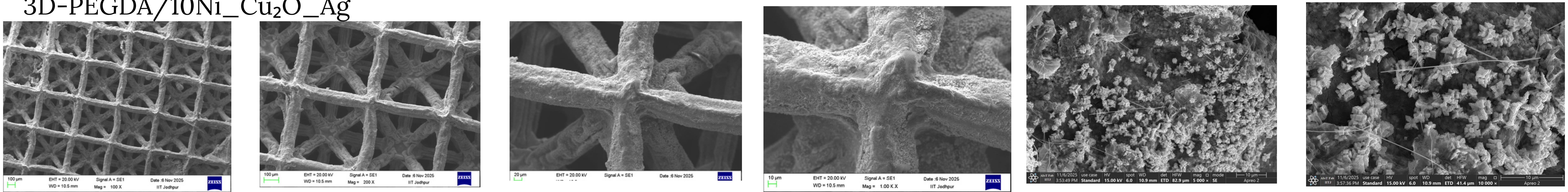

EDS

3D-PEGDA/0.5Ni_Cu_2O

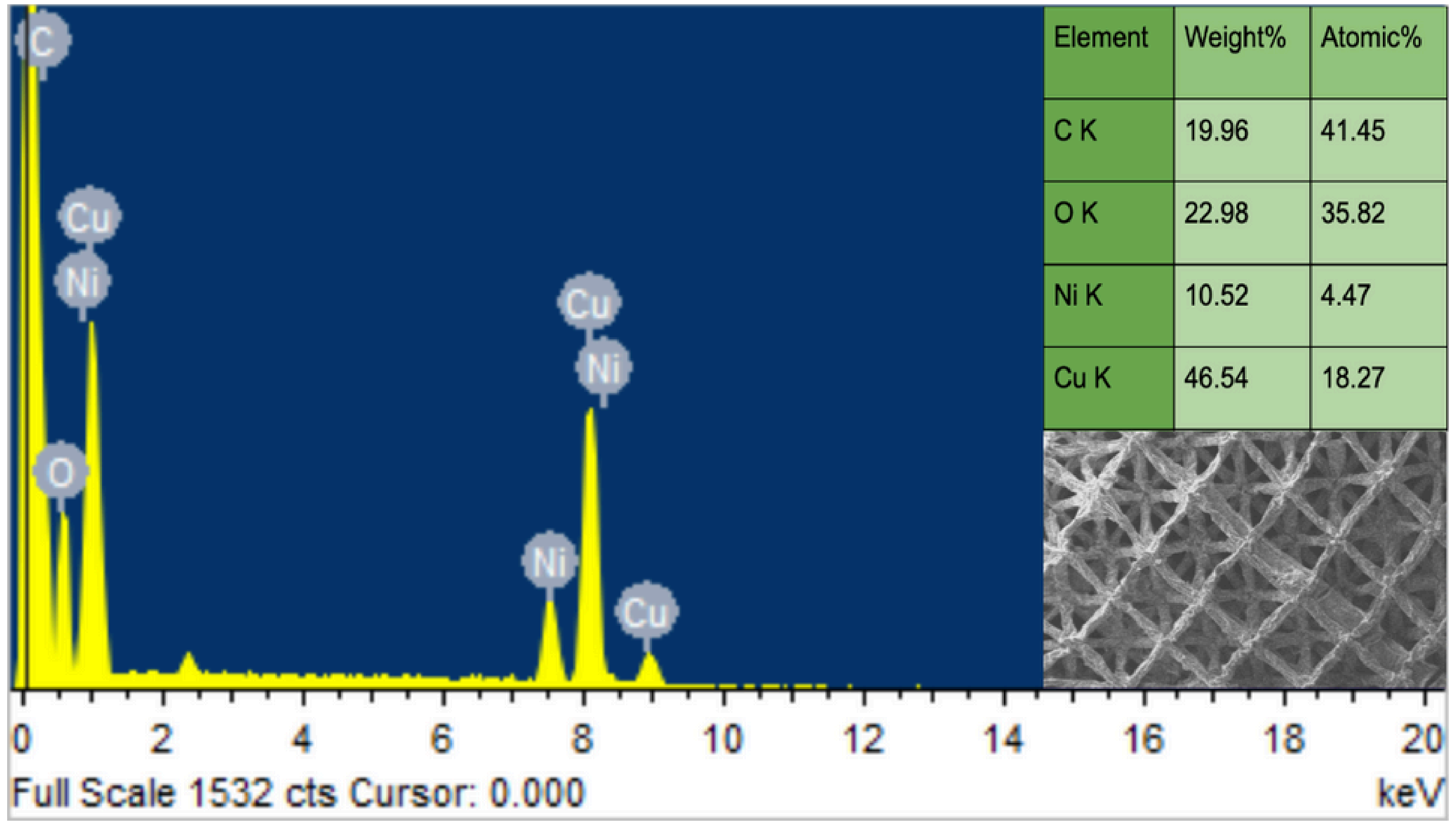

Element	Weight%	Atomic%
C K	19.96	41.45
O K	22.98	35.82
Ni K	10.52	4.47
Cu K	46.54	18.27

3D-PEGDA/1Ni_Cu_2O

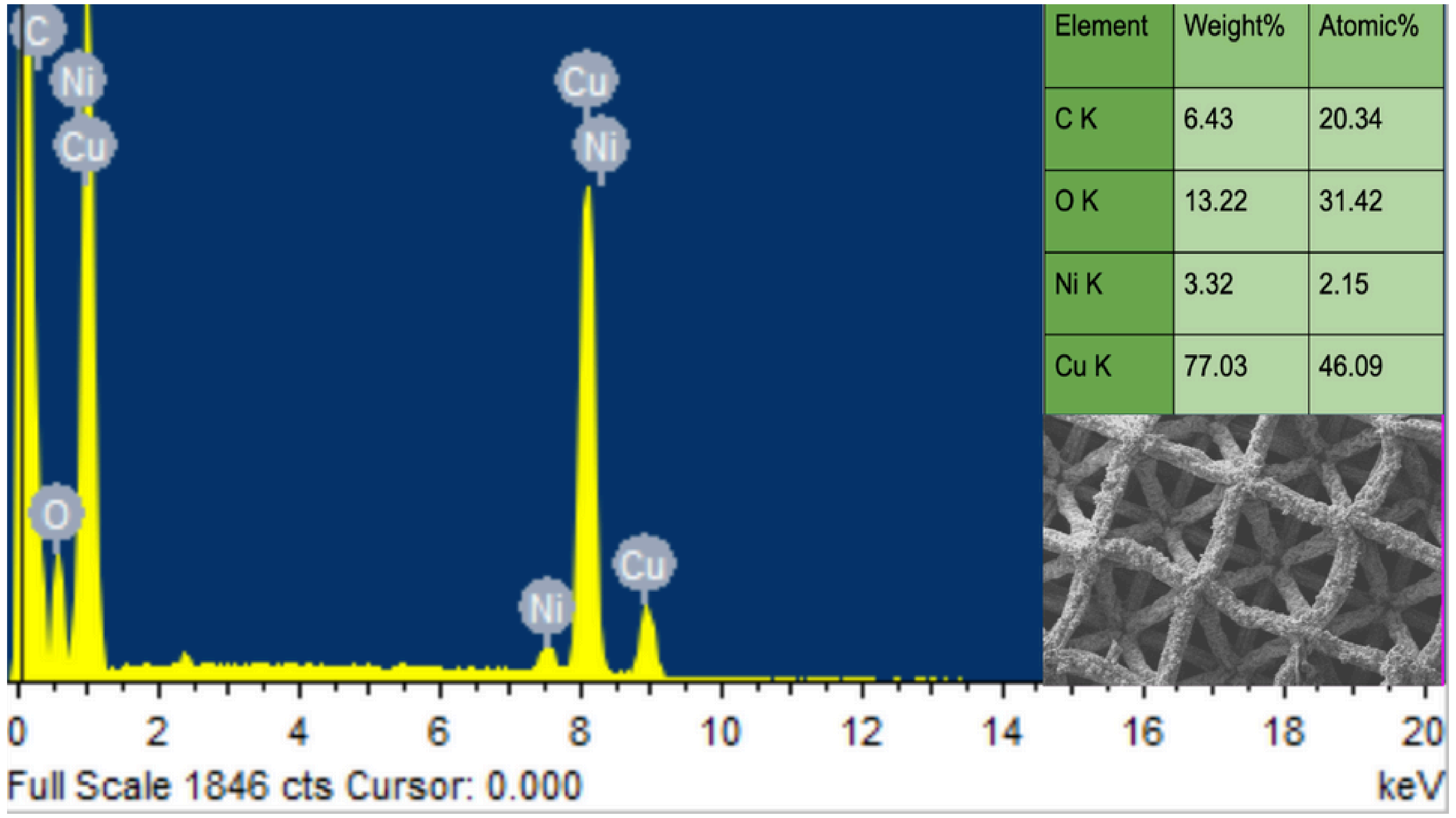

Element	Weight%	Atomic%
C K	6.43	20.34
O K	13.22	31.42
Ni K	3.32	2.15
Cu K	77.03	46.09

EDS

3D-PEGDA/0.5Ni_Cu_2O_Ag

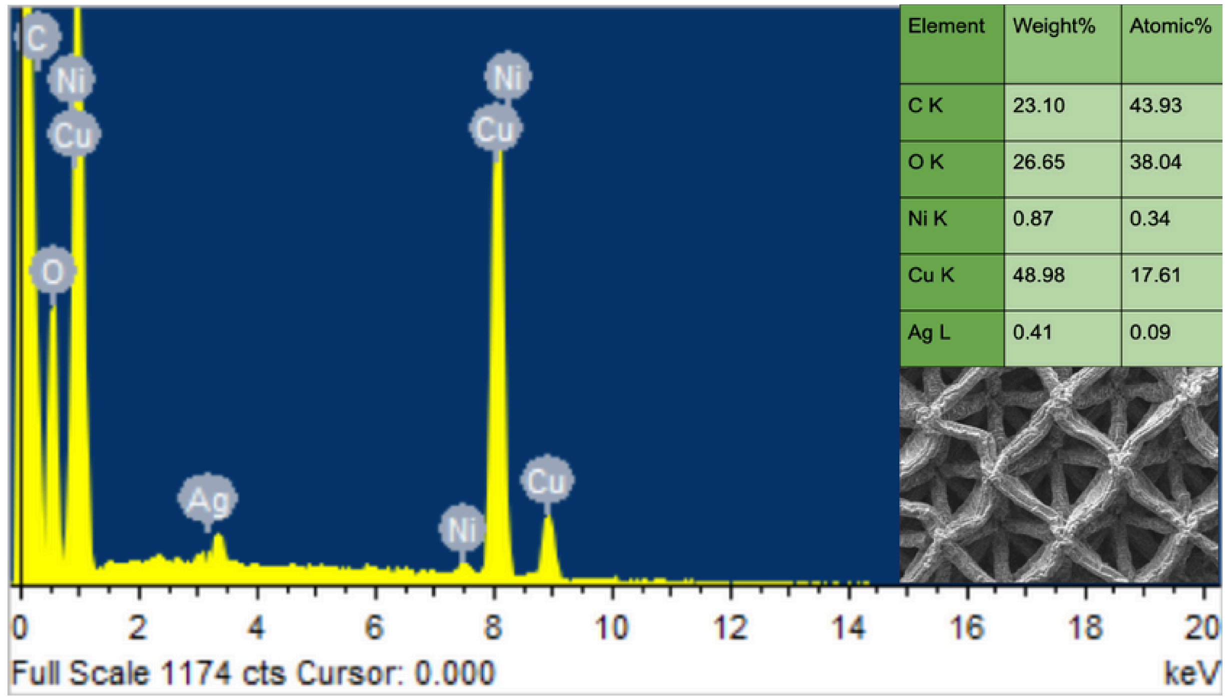

Element	Weight%	Atomic%
C K	23.10	43.93
O K	26.65	38.04
Ni K	0.87	0.34
Cu K	48.98	17.61
Ag L	0.41	0.09

3D-PEGDA/1Ni_Cu_2O_Ag

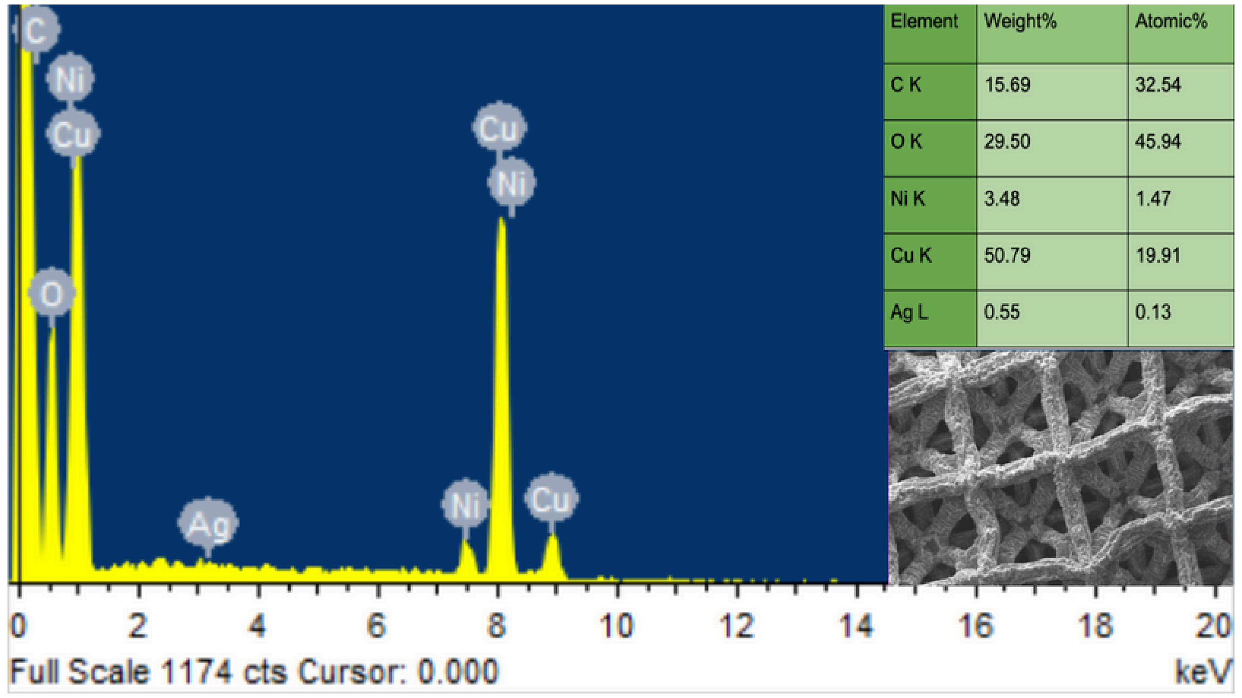

Element	Weight%	Atomic%
C K	15.69	32.54
O K	29.50	45.94
Ni K	3.48	1.47
Cu K	50.79	19.91
Ag L	0.55	0.13

3D-PEGDA/5Ni_Cu_2O_Ag

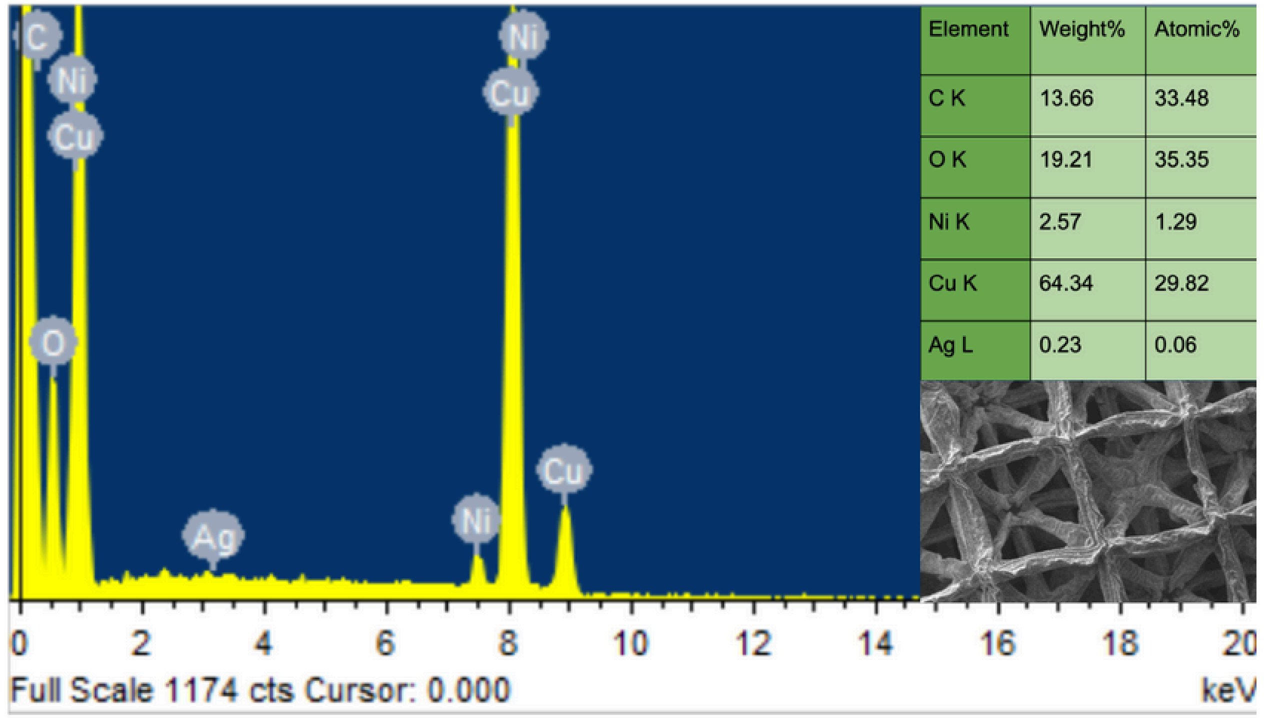

Element	Weight%	Atomic%
C K	13.66	33.48
O K	19.21	35.35
Ni K	2.57	1.29
Cu K	64.34	29.82
Ag L	0.23	0.06

3D-PEGDA/10Ni_Cu_2O_Ag

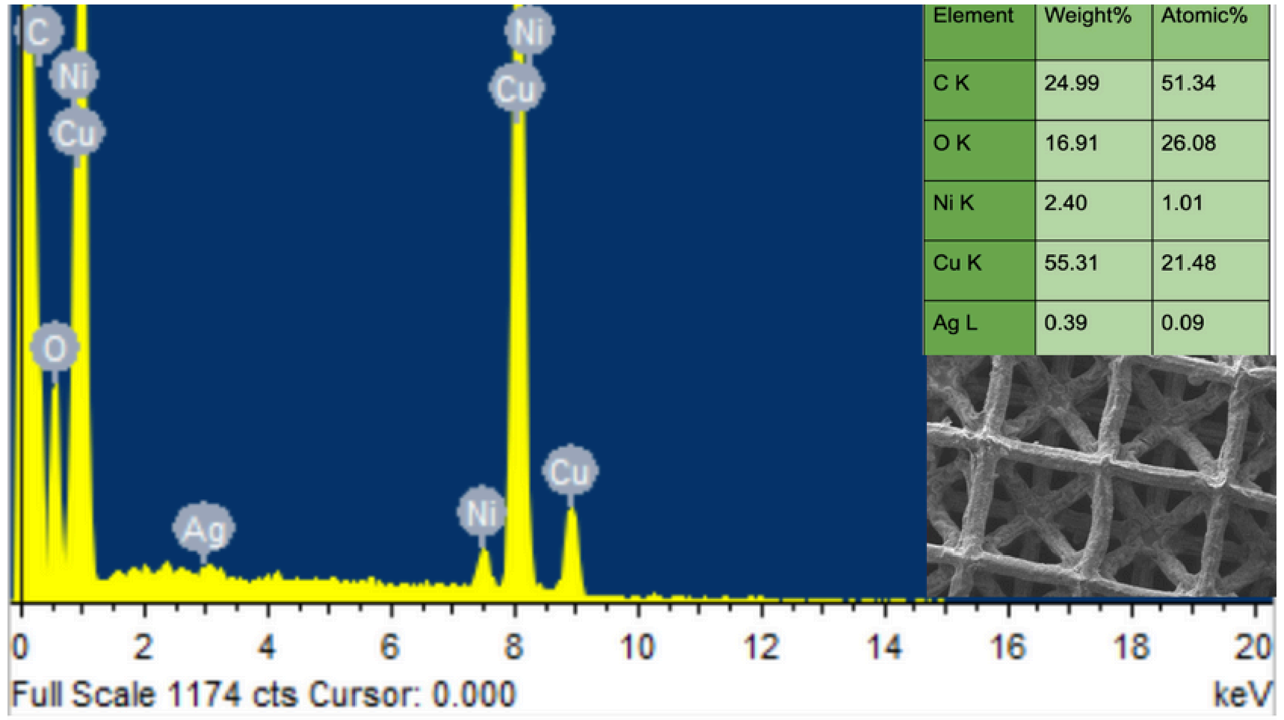

Element	Weight%	Atomic%
C K	24.99	51.34
O K	16.91	26.08
Ni K	2.40	1.01
Cu K	55.31	21.48
Ag L	0.39	0.09

3D-PEGDA/0.5Ni_Cu_2O

3D-PEGDA/1Ni_Cu_2O

3D-PEGDA/5Ni_Cu_2O

3D-PEGDA/10Ni_Cu_2O

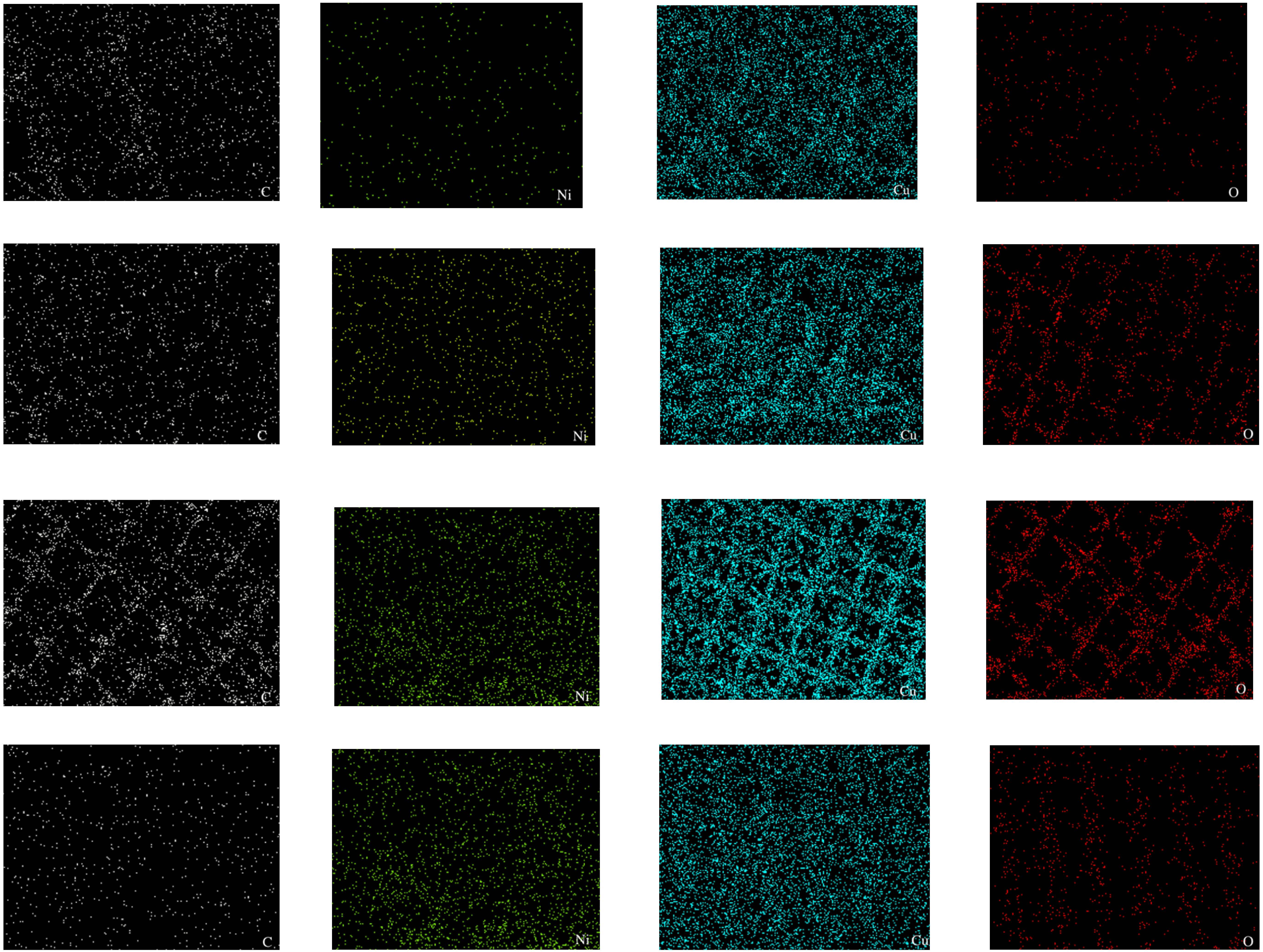

3D-PEGDA/0.5Ni_Cu_2O_Ag

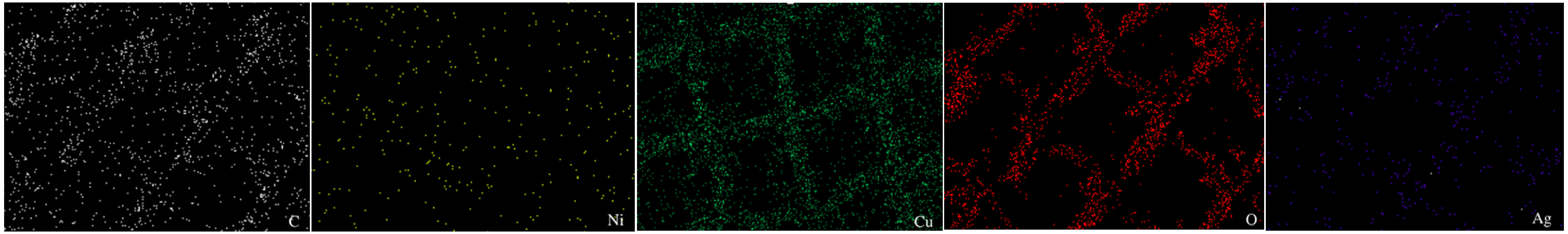

3D-PEGDA/1Ni_Cu_2O_Ag

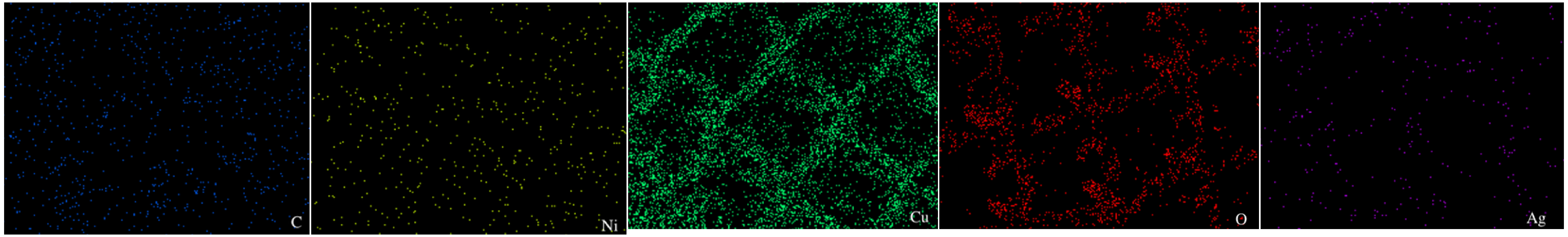

3D-PEGDA/5Ni_Cu_2O_Ag

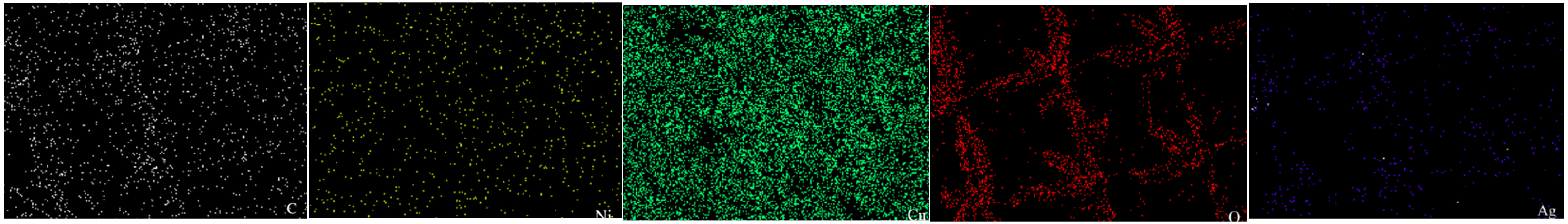

3D-PEGDA/10Ni_Cu_2O_Ag

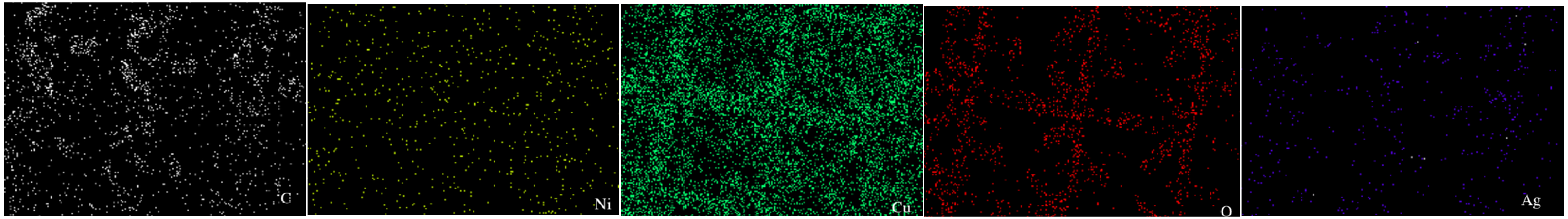

Looking at the EDS color mapping, it is clear that Cu deposition is highest in the 5% Ni sample.

The Cu signal appears denser and more uniformly spread at 5% Ni compared to 0.5%, 1%, and 10% Ni.

XRD

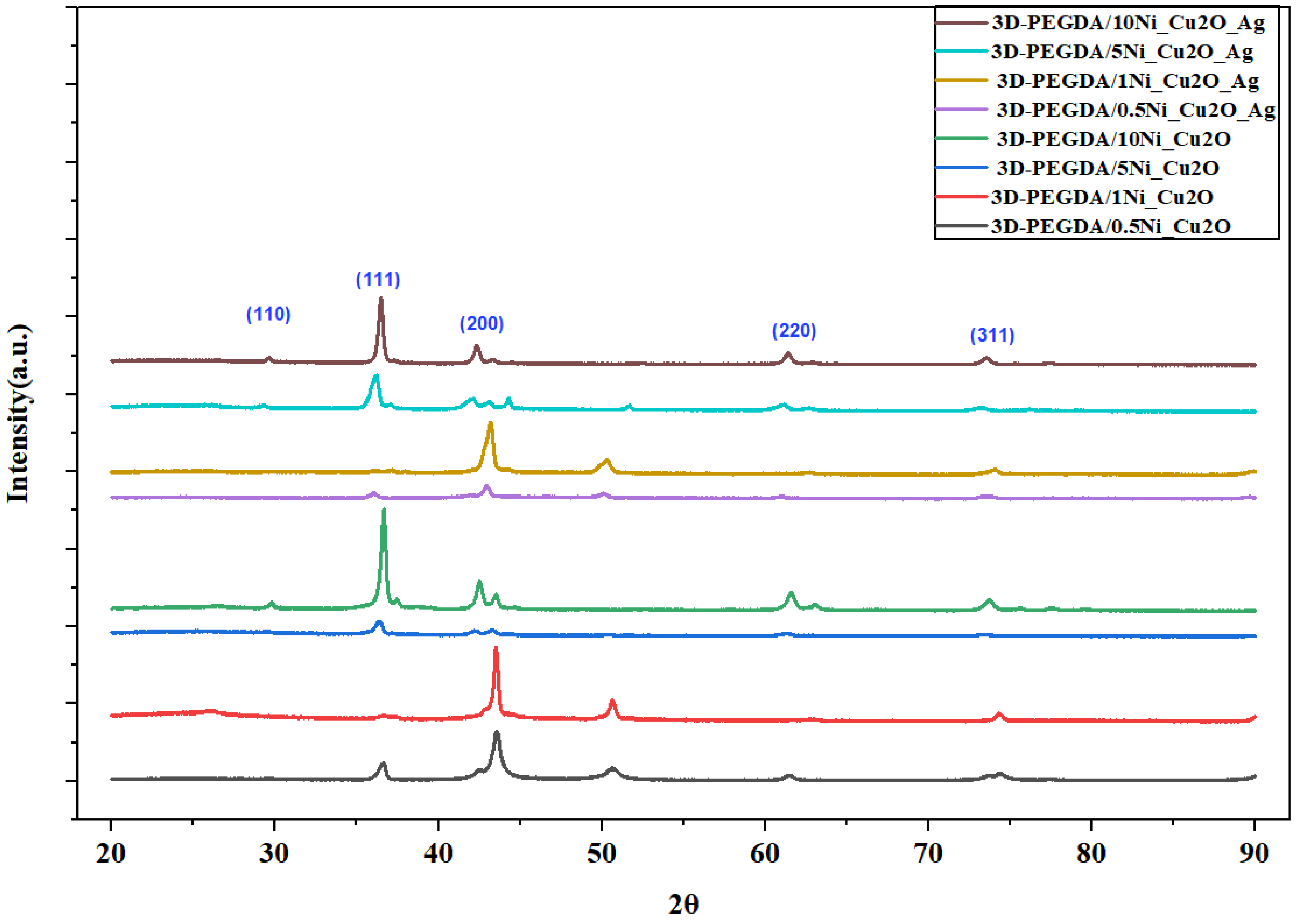

◆ Cu_2O Formation

- XRD shows strong reflections at ~30°, 36°, 42°, 62°, 73°
- These match standard Cu_2O peaks → confirms Cu_2O deposition on all samples

◆ Ag Detection

- Additional peaks appear around 38°, 44°, 64° only in Ag-coated samples
- Low intensity → Ag deposited in small amount or finely dispersed

◆ Influence of Ni Content

- As Ni increases, peaks become sharper and more defined
- Indicates better crystal growth and higher structural order

Raman Spectroscopy

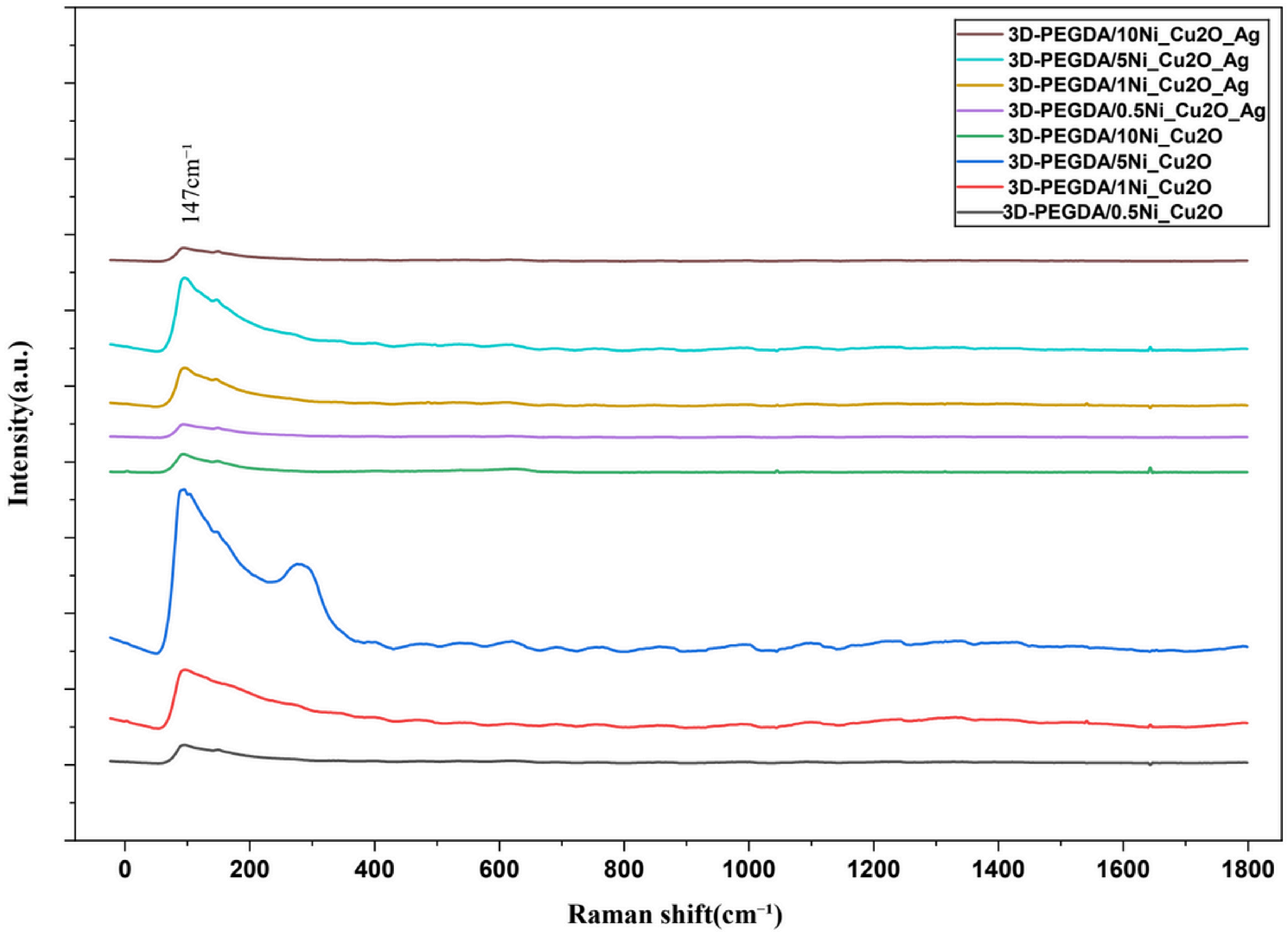

The symmetric stretching of oxygen atoms in the cuprite crystal lattice produces a Raman-active vibrational mode that is highly ordered and strong, appearing around ~150 cm^{-1}. Therefore, the peak observed at ~147 cm^{-1} confirms the presence of Cu_2O.

We observe that as Ni increases, Cu_2O formation increases up to 5% Ni and then decreases at 10%.

This is reflected by the highest Raman intensity at 5% Ni, followed by a clear drop at 10% Ni.

Observation

CuO/Cu_2O 5 Ni sample

T = 30 Min T = 60 Min T = 90 Min T = 120 Min T = 150 Min T = 180 Min

Reduction in MB Concentration

CuO/Cu_2O 5 Ni sample with Ag

T = 30 Min T = 60 Min T = 90 Min T = 120 Min T = 150 Min T = 180 Min

Observation

- From SEM we can observe that Cu_2O appears as a rough, granular coating on the PyC struts, forming small clustered deposits that clearly indicate successful nucleation and surface coverage.

- Ag nanowires or **thin flake-like features are clearly visible** decorating the Cu_2O layer, especially around the joints and intersections of the struts.

- Among all samples, the **5% Ni sample shows the highest and most uniform Cu-based deposition,** as seen from the denser Cu distribution and stronger structural signals compared to 0.5%, 1%, and 10% Ni.

- The crystalline features associated with Cu_2O are strongest at 5% Ni, indicating that this **Ni content promotes better nucleation and growth of Cu_2O**, while 10% Ni causes a decline due to unstable deposition conditions.

- A clear Raman peak around ~147–150 cm^{-1}, arising from symmetric stretching of oxygen atoms in the cuprite lattice, confirms the presence of Cu_2O, and the intensity of this peak is also highest at 5% Ni.

- All characterization techniques consistently show a trend: **Cu_2O formation increases from 0.5% → 1% → maximum at 5% Ni, followed by a drop at 10% Ni**, indicating an optimal Ni level for stable and uniform oxide growth.

- This trend directly reflects in performance, with the **5% Ni sample showing the maximum Methylene Blue degradation**, correlating with its highest Cu_2O loading, best crystallinity, and most uniform surface coverage.

Conclusion

Cu_2O Deposition Increases Progressively from 0.5% to 5% Ni

- As Ni content increases from 0.5% to 5%, Cu_2O deposition increases steadily because the surface gains more Ni sites that improve electron-transfer efficiency.
- More Ni provides additional high-energy nucleation sites, allowing Cu_2O crystals to start forming more easily and in larger numbers.
- Ni helps maintain a more stable local pH during electrodeposition, which supports proper Cu_2O growth instead of patchy or discontinuous films.
- Together, these effects lead to faster Cu^{2+} reduction, higher nucleation density, and more uniform Cu_2O crystal growth, resulting in maximum Cu_2O deposition at 5% Ni.

Conclusion

Cu_2O Formation Drops at Higher Ni Content

Reasons

1) High Ni makes the surface too conductive
- Fast electron flow pushes the potential very negative.
- This favors $Cu^{2+} \rightarrow Cu^0$ (metal), not Cu_2O formation. But metallic Cu does not deposit uniformly → overall Cu deposition decreases.

2) Ni catalyzes the Hydrogen Evolution Reaction (HER)

Reaction: $H^+ + e^- \rightarrow H_2$
- HER competes with Cu deposition.
- H_2 bubbles block the surface → Cu ions can't reach the surface properly.

Result → reduced Cu deposition.

3) Local pH becomes unstable near the surface

HER increases OH^- concentration suddenly.

The unstable pH conditions disrupt Cu_2O formation.

Instead of depositing, some Cu redissolves or forms uneven spots → less net Cu deposited.

So,Cu_2O deposition increases steadily from 0.5% to 5% Ni due to improved nucleation and electron transfer, but drops at 10% Ni because excessive Ni disrupts stable Cu_2O growth.

Conclusion

- Among all the samples tested, the composite containing 5% Ni exhibited the highest photocatalytic activity, showing the most visible and significant degradation of methylene blue. This indicates that 5% Ni loading provides the optimum balance between active surface sites and charge-transfer efficiency, leading to enhanced dye breakdown under the given experimental conditions.

- There was no significant visible difference in the cleaning efficiency between samples prepared with Ag and those without Ag. Since Ag was drop-casted, the deposited material dissolved immediately upon contact with the solution, preventing any meaningful comparison of their surface-assisted degradation performance.